ISSN 1027-5495. Functional Materials, 26, No.4 (2019), p. 829-837.
doi:https://doi.org/10.15407/fm26.04.829

Y_2O_3–MgO highly-sinterable nanopowders for transparent composite ceramics

***O.S.Kryzhanovska*[1], *N.A.Safronova*[1], *A.E.Balabanov*[1], *R.P.Yavetskiy*[1], *M.V.Dobrotvorskaya*[1], *Jiang Li*[2], *S.Petrushenko*[3], *A.V.Tolmachev*[1], *N.A.Matveevskaya*[1], *E.N.Shulichenko*[3], *V.Yu.Mayorov*[4], *D.Sofronov*[5]**

[1]Institute for Single Crystals, STC "Institute for Single Crystals", National Academy of Sciences of Ukraine, 60 Nauky Ave., 61072 Kharkiv, Ukraine
[2]Key Laboratory of Transparent Opto-functional Inorganic Materials, Shanghai Institute of Ceramics, Chinese Academy of Sciences, 201899 Shanghai,China
[3]V.Karazin Kharkiv National University, 4 Svobody Sq., 61022 Kharkiv, Ukraine
[4]Institute of Chemistry, Far Eastern Branch, Russian Academy of Sciences, 159 100-let Vladivostoku Avenue, 690022 Vladivostok, Russian Federation
[5]SSI "Institute for Single Crystals", STC "Institute for Single Crystals", National Academy of Sciences of Ukraine, 60 Nauky Ave., 61072 Kharkiv, Ukraine

Received May 11, 2019

Composite nanopowders Y_2O_3–MgO (1:1 by volume) were synthesized by the method of self-propagating glycine-nitrate synthesis with an excess of glycine and nitric acid. It was shown that freshly prepared powder (precursor) contains about 19 % of unreacted components and intermediate reaction products, which are removed by subsequent calcining. Crystallization of the precursor starts at calcination temperature above 600°C and leads to nucleation of the crystalline phases MgO and Y_2O_3. It was shown that calcining at temperatures from 800 to 1000°C leads to the formation of nanocrystals with sizes from 20 to 90 nm, respectively. The specific surface area of composite nanopowders decreases from 48 to 16 m^2/g with increasing calcination temperature in the range T = 700–1000°C. It was shown that during Y_2O_3–MgO calcination in the air, intense chemisorption of CO_2 occurs on the surface of nanopowders. According to calculations, about 5 % of MgO is converted to magnesium carbonate. Finally, Y_2O_3–MgO composite ceramics with average grain size of 255 nm and transmittance of 71 % at λ = 6000 nm have been obtained by spark plasma sintering of synthesized nanopowders.

Keywords: nanopowders, self-propagating glycine-nitrate synthesis, composite ceramics, magnesium oxide, yttrium oxide.

Методом самораспространяющегося глицин-нитратного синтеза с избытком глицина и азотной кислоты синтезированы композитные нанопорошки Y_2O_3–MgO (1:1 по объему). Показано, что свежеприготовленный порошок (прекурсор) содержит около 19 % непрореагировавших компонентов и промежуточных продуктов реакции, которые удаляются последующим отжигом. Кристаллизация прекурсора происходит при температуре про-

каливания выше 600°C и приводит к нуклеации кристаллических фаз MgO и Y_2O_3. Показано, что прокаливание при температурах от 800 до 1000°C приводит к формированию нанокристаллов с размерами от 20 до 90 нм, соответственно. Удельная площадь поверхности композитных нанопорошков снижается с 48 до 16 $м^2/г$ с повышением температуры отжига в диапазоне T = 700–1000°C. Показано,что в процессе прокаливания Y_2O_3–MgO в воздушной атмосфере происходит интенсивная хемосорбция CO_2 на поверхности нанопорошков. В соответствии с расчетами, порядка 5 % MgO переходит в карбонат магния. Методом плазменно-искрового спекания из синтезированных порошков получена композитная керамика Y_2O_3–MgO со средним размером зерна 255 нм и пропусканием 71 % при λ = 6000 нм.

Нанопорошки Y_2O_3–MgO для прозорої композитної кераміки. *О.С.Крижановська, Н.А.Сафронова, А.Е.Балабанов, Р.П.Явецький, М.В.Добротворська, Цзян Лі, С.Петрушенко, О.В.Толмачов, Н А.Матвєєвська, О.М.Шуліченко, В.Ю.Майоров, Д.Софронов.*

Методом самопоширюваного гліцин-нітратного синтезу з надлишком гліцину і азотної кислоти синтезовано композитні нанопорошки Y_2O_3–MgO (1:1 за об'ємом). Показано,що свіжоприготований порошок (прекурсор) містить близько 19 % компонентів, що не прореагували, і проміжних продуктів реакції, які видаляються наступним відпалом. Кристалізація прекурсора відбувається при температурі прожарювання вище 600°C і приводить до нуклеації кристалічних фаз MgO і Y_2O_3. Показано, що прожарювання при температурах від 800 до 1000°C приводить до формування нанокристалів з розмірами від 20 до 90 нм, відповідно. Питома площа поверхні композитних нанопорошків знижується з 48 до 16 $м^2/г$ з підвищенням температури відпалу у діапазоні T = 700–1000°C. Показано, що у процесі прожарювання Y_2O_3–MgO в повітряній атмосфері відбувається інтенсивна хемосорбція CO_2 на поверхні нанопорошків. Відповідно до розрахунків, близько 5 % MgO переходить у карбонат магнію. Методом плазмово-іскрового спікання з синтезованих порошків отримано композитну кераміку Y_2O_3–MgO із середнім розміром зерна 255 нм і пропусканням 71 % при λ = 6000 нм.

1. Introduction

The transparent composite nanoceramics Y_2O_3–MgO is being actively studied as a promising material for IR optics. Y_2O_3–MgO nanocomposite has much better optical and mechanical properties, in comparison with a single-phase counterparts [1, 2].

To create such ceramics, controlled dispersion nanopowders are used, which are compacted using high-speed consolidation methods, such as hot pressing (HIP) and spark plasma sintering (SPS). These methods are designed to suppress diffusion mass transfer in order to prevent grain growth above 400 nm. The submicron grain size and their uniform distribution in the ceramic volume provide high hardness and strength along with high optical properties. A number of methods are used to prepare starting powders, such as spray pyrolysis, coprecipitation, sol-gel, hydrothermal [3–7]. Solution combustion synthesis (SCS) stands out among them. It is based on a fast and self-sustained redox reaction between fuel and an oxidant in the presence of metal cations resulting in metals oxides nanopowder formation [8, 9]. Particle diameter and size distribution, surface condition, specific surface area and porosity depend on many SCS parameters, the main of which is the composition of oxidant-fuel mixture. It is usually expressed in terms of elements stoichiometric coefficient (Φ_e) [8]. Optimization of the conditions for obtaining nanopowders to increase their sinterability is reduced to fine tuning of the size of nanoparticles and the values of their specific surface area by varying the parameter Φ_e, pH of the solution, and subsequent calcining temperature [10–13]. A characteristic feature of high-speed consolidation methods is extremely high sintering speed. Therefore, the use of extremely small Y_2O_3–MgO nanopowders leads to the pores formation in ceramics, because the high sintering ability of finely dispersed powders leads to the rapid closure of internal pores, which are not removed during further compaction [14].

The preparation of deagglomerated particles is a key point in compaction using the SPS method. To obtain homogeneous ceramics with 100 % relative density and high optical properties, it is necessary to minimize temperature gradients in the compact volume during sintering. A uniform distribution of the contact points of particles on which energy dissipation occurs, and interparticle spaces, in which local heating will occur, ensure this. Thus, conditions when compaction is carried out mainly due to plastic deformation, avoiding grain-bound-

ary sliding, rotations and subsequent coalescence of grains, are created.

One of the methods of high-temperature self-propagating synthesis is the glycine-nitrate method. It is simple, well adapted for use in hot pressing [10, 12] and allows to obtain nanoparticles in a wide range of sizes and specific surface area depending on combustion conditions. The use of reaction systems with an excess of glycine allows to generate a large number of nucleation sites in the synthesis process in a short period of time, ensuring a small size distribution of nanoparticles, while the release of large volumes of gases ensures particle agglomeration. Thus, the glycine-nitrate synthesis method is promising for the production of Y_2O_3–MgO nanopowders and its adaptation for compacting ceramics by the SPS method is of current interest.

2. Experimental

Synthesis of Y_2O_3–MgO nanopowders and composite ceramics

Yttrium oxide Y_2O_3 (99.999 %, Alfa Aesar) and magnesium oxide MgO (99.99 %, Alfa Aesar) powders were dissolved in nitric acid HNO_3 (69 %, Fluka Trace Select), taken in proportion 1:1 by volumes of the final oxides, to form $Y(NO_3)_3$ and $Mg(NO_3)_2$ solution. Glycine deionized water solution $C_2H_5NO_2$ (99 %, Merck) was added to $Y(NO_3)_3$ and $Mg(NO_3)_2$ solution in a molar ratio corresponding to stoichiometry of redox-reactions (1–3) taking into account the excess of nitric acid (5 %) used to dissolve the oxides.

$$Mg(NO_3)_2 + C_2H_5NO_2 = MgO + CO_2 + H_2O + N_2, \quad (1)$$

$$Y(NO_{3)_3} + C_2H_5NO_2 = Y_2O_3 + CO_2 + H_2O + N_2, \quad (2)$$

$$HNO_3 + C_2H_5NO_2 = CO_2 + H_2O + N_2. \quad (3)$$

The oxidant-fuel mixture that is usually expressed in terms of elements stoichiometric coefficient (Φ_e), was calculated using Eqs. (2) and (3) [15].

$$\Phi_e = \frac{\sum(C_{oxi})\cdot(v)}{(-1)\sum(C_{red})\cdot(v)}, \quad (4)$$

where C_{oxi} is the coefficient of oxidizing elements; C_{red} is the coefficient of reducing elements; v is the valency. $\Phi_e = 1$ corresponds to the stoichiometric ratio, $\Phi_e > 1$ indicates a fuel lean system and $\Phi_e < 1$ is a fuel rich system. The valence ratio value in this work was 0.83 that corresponded to fuel rich system.

Obtained solution was stirred and heated to boiling. After water evaporation, solution transformed to gel which self-ignited at approximately 200°C forming precursor powder. Precursor was calcined in air at 600, 800, 1000°C for 4 h in order to produce Y_2O_3–MgO nanopowders.

Sintering experiments were conducted using a SPS-515S (Dr. Sinter*LAB, Japan) unit at 1300°C for 8 min at the pressure 50 MPa and average heating rate of 100°C/min.

Characterization of Y_2O_3–MgO nanopowders and composite ceramics

Simultaneous thermogravimetric and differential scanning calorimetric (TGA/DSC) analysis was performed on NETZSCH 449C thermal analyzer at a heating rate of $10°C\cdot min^{-1}$. Powder X-ray diffraction (XRD) studies were performed on Shimadzu XRD 6100 (Japan) diffractometer using CuKα radiation (1.54060 Å). Fourier transform infrared spectra (FT-IR) of the samples were measured on a FT-IR spectrometer SPECTRUMONE (PerkinElmer) with the KBr pellet technique. Field emission scanning electron microscopy (FESEM, Model Magellan-400, FEI, USA) and transmission electron microscopy (TEM, TEM-125, Selmi, Ukraine) were used to evaluate morphology of the nanopowders.

Specific surface area (S), average pore diameters (D_{np}) and total pore volumes (V_{Tp}) of the prepared Y_2O_3–MgO nanopowders were calculated from N_2 physisorption data using "Autosorb IQ" automated gas analyzer (Quantachrome Instruments). Calculations were conducted by Brunauer-Emmett-Teller (BET), Barrett-Joyner-Halenda (BJH) and Density Functional Theory (DFT) methods using standard Quadrasorb SI software. All samples were degassed at 100°C for 12 h to remove any physically adsorbed species.

Average particle size was evaluated from S:

$$d = \frac{F_S}{\rho S}\cdot 10^9, \quad (5)$$

where ρ is the density of the material (g/m^3), S is the specific surface area of the

material (m^2/g), F_S is the shape factor of the particles (6 for cubes and spheres) [16].

The transmittance of 1 mm-thick polished samples of Y_2O_3–MgO composite ceramics were studied using a Fourier-Transform Infrared (FTIR) spectrometer (Vertex-80, Bruker Optik GmbH, Germany).

3. Results

Dependence of the composition and morphology of composite nanopowders Y_2O_3–MgO on the calcination temperature

Fig. 1 shows the thermogravimetric and DTA curves of freshly synthesized uncalcined Y_2O_3–MgO powder. Mass loss at temperatures up to 225°C is associated with removal of absorbed and molecular water (about 8 % of the mass). In the range from 225 to 650°C the mass loss is 19 % due to the decomposition of the intermediate phases and the starting components that did not react during the synthesis. The endothermic peak on the DTA curve at about 405°C corresponds to pyrolysis of yttrium nitrate [17] and magnesium glycinate [18], the exothermic peak at 561°C corresponds to decomposition of $YOHCO_3$ phase [19].

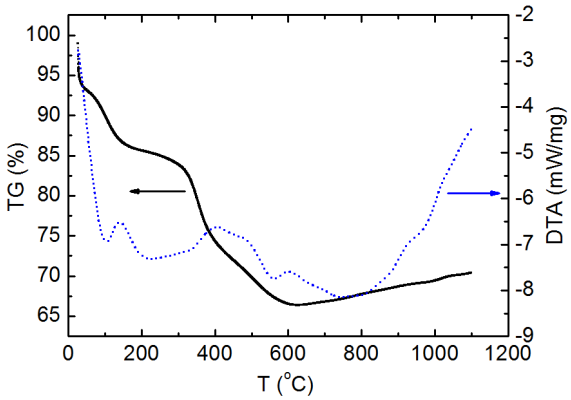

Fig. 1. Thermogravimetric and DTA curve of Y_2O_3–MgO precursor.

Above 600°C, continuous mass gain is observed, which reaches 3.66 % at 1100°C, apparently associated with adsorption of CO_2 by the surface of nanopowders from purged air. A similar mass gain was observed in [20] at temperatures above 750°C with thermogravimetry of the olivine mineral containing 35 % MgO.

According to transmission electron microscopy, the synthesized Y_2O_3–MgO powder

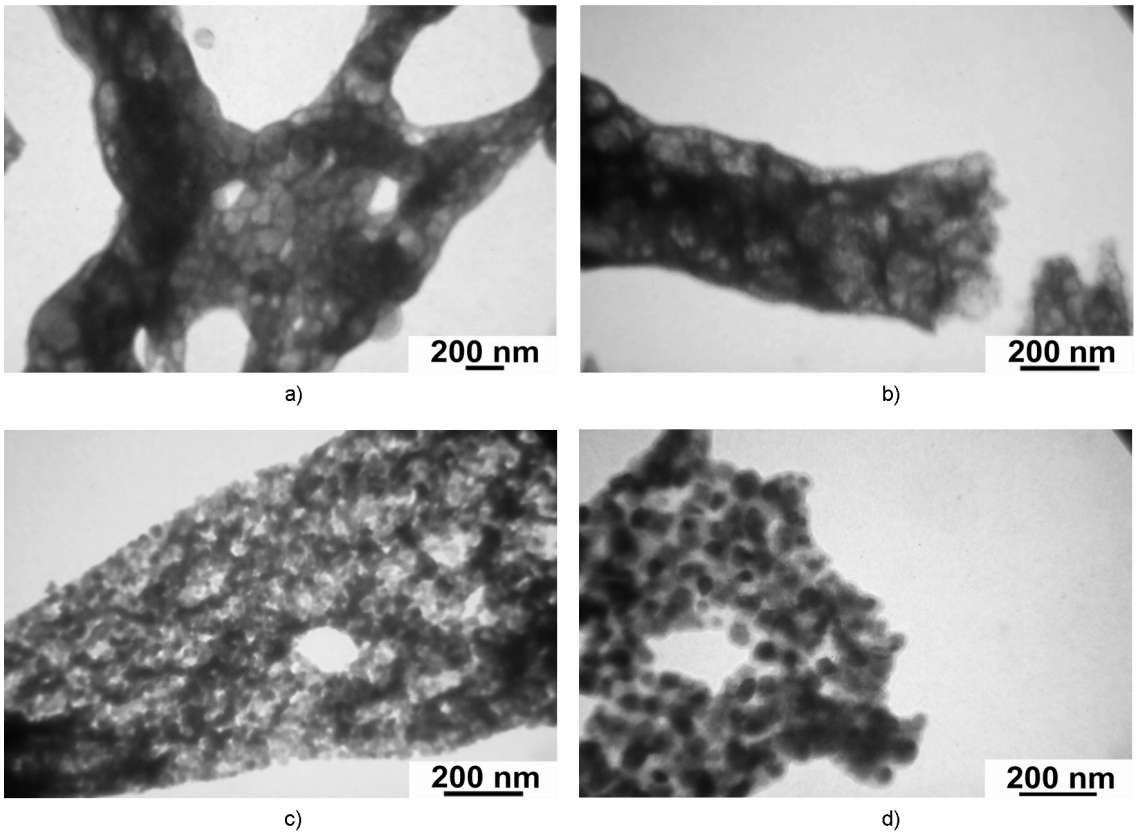

Fig. 2. TEM images of Y_2O_3–MgO precursor (a) and nanopowders calcined at 600 (b), 800 (c) and 1000°C (d) for 2 h.

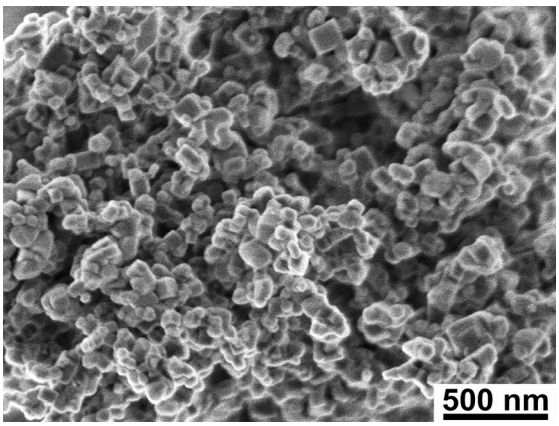

Fig. 3. FESEM image of Y_2O_3–MgO nanopowders calcined at 1000°C for 4 h.

is a foam (porous gel) (Fig. 2a). After calcining at 600°C for 2 h, the powder is a branched fiber with thickness of less than 10 nm, reproducing the structure of the initial gel (Fig. 2b). It can be seen that spaces between fibers are hollow, which is associated with the removal of gaseous water and organic components of the powder, as well as with decomposition of the unreacted part of nitrates and carbonates. This correlates with total mass loss of 26.7 %. Calcination at 800°C leads to the formation of isolated nanoparticles with size about 20 nm (Fig. 2c). Higher mass loss compared to 600°C (32.8 %) is apparently associated with the complete decomposition of residual unreacted components. The average nanocrystal size in powder calcined at 1000°C is 59 nm (Fig. 2d). Despite the significant enlargement of particles, the mass loss during calcining is less than at 800°C (30.65 %), which may be associated with the adsorption of gases from air during powder cooling. According to FESEM, Y_2O_3–MgO nanopowder, calcined at 1000°C, represents agglomerates up to 1 μm in size, consisting of cubic nanoparticles with size of 80–100 nm (Fig. 3).

XRD pattern of the powder annealed at 600°C contains the main reflections corresponding to the phases of cubic MgO (space group *Fm3m*, JCPDS No. 45-0946) and cubic Y_2O_3 (space group *Ia3*, JCPDS No. 41-1105) (Fig. 4a). The lines are significantly broadened, which indicates small crystallite size. With increasing calcination temperature, the lines become narrow, their intensity increases, which indicates an increase in crystallite sizes. XRD pattern of the powder calcined at 1000°C shows that it consists of crystalline phases of magnesium oxide and yttrium oxide, impurity phases were not detected within the sensitivity of the method. Thus, the powder is a homogeneous mixture of isolated MgO and Y_2O_3 nanocrystals.

Fig. 4b demonstrates FT-IR transmission spectra of as-prepared and calcined Y_2O_3–MgO nanopowders. The absorption broad band centered at 3430 as well as 1634 cm^{-1} and 1019 should be attributed to O–H stretching and bending vibrations, respectively [21, 22]. The bands in the interval from 1330 to 1740 cm^{-1} can be attributed to different species of carbonates. The intensity of this group of lines is almost the same for all calcined powders. The bands appeared at low frequency of 560 cm^{-1} correspond to stretching vibration of Me–O–Me bonding. The intensity of these lines increases with increasing calcination temperature. The absorption spectrum of the uncalcined powder contains a narrow line at 1385 cm^{-1}, corresponding to asymmetric

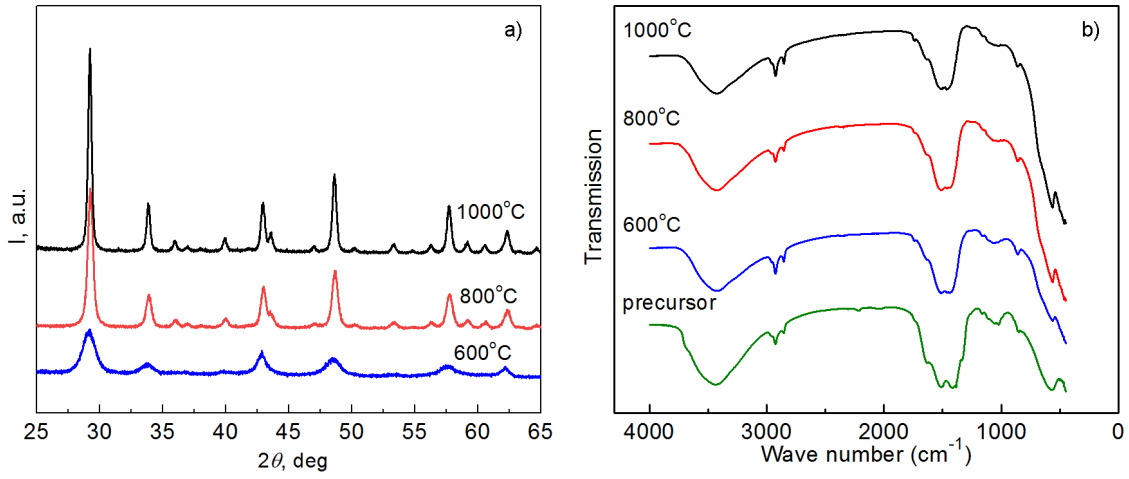

Fig. 4. XRD (a) and FT-IR patterns (b) of Y_2O_3–MgO nanopowders calcined at 600, 800 and 1000°C.

stretching vibration of the NO_3^- [23] group, which disappears after calcination.

A more detailed study of the powders structure was carried out by the volumetric statistical method of nitrogen adsorption capacity. The nitrogen adsorption isotherms of Y_2O_3–MgO powders calcined at 700, 800, and 900°C for 4 h are shown in Fig. 5a. The form of isotherms is of type IV according to the IUPAC classification, which corresponds to capillary condensation in mesopores. On the adsorption-desorption graph, 1H type hysteresis loop is observed, which corresponds to the globular shape of the particles [16]. The specific surface area of composite powders decreases with increasing calcination temperature from 48 to 16 m^2/g, which corresponds to an increase in particle size from 30 to 90 nm (Table). The average pore diameter and total porosity of the powders were determined by BJH and DFT methods. With increasing calcination temperature, the average pore diameter increases, and the porosity decreases. The Table shows that these values are in good agreement for samples obtained at relatively low temperatures. The mismatch at high temperatures does not violate the general tendency and is explained by the features of the methods. The pore size distribution obtained by two different methods is shown in Fig. 5b, c. With increasing calcination temperature, the main maximum of the pore distribution shifts to the region of large diameters. In addition, at calcination temperatures of 800 and 900°C, new pores with diameter of less than 5 nm appear.

Optical properties of SPS sintered Y_2O_3–MgO composite ceramics

To study sinterability of obtained powders, Y_2O_3–MgO powders calcined at different temperatures were subjected to consolidation by SPS method at T = 1300°C. The powders were loaded into a graphite die with an inner diameter of 15 mm, the internal surface of which was covered with graphite sheet.

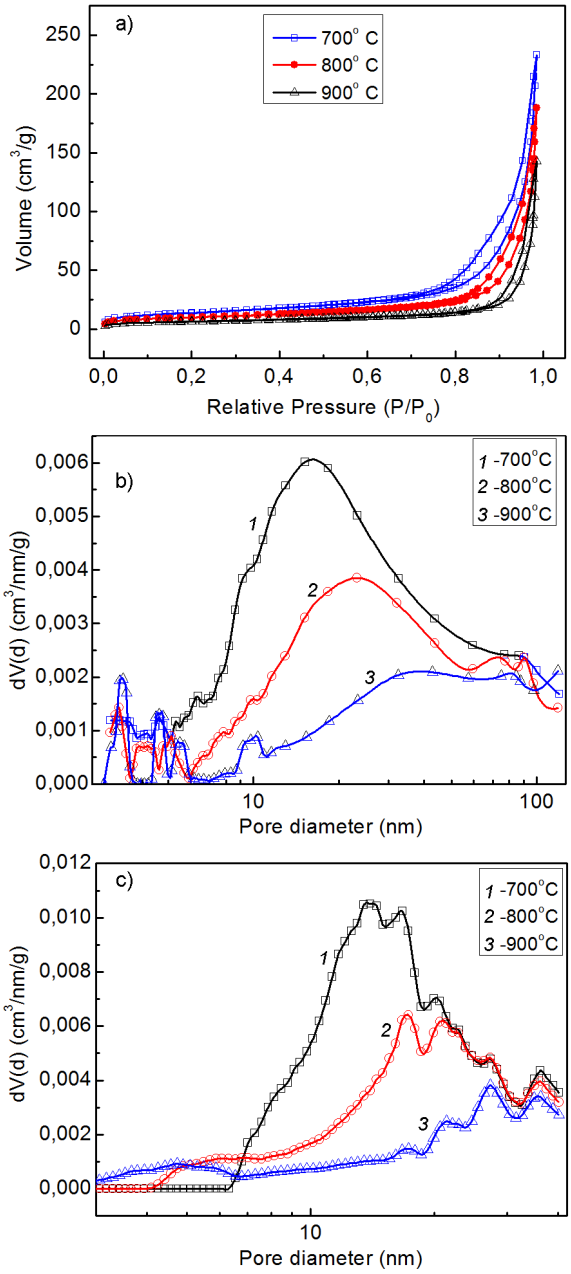

Fig. 5. Adsorption isotherms of Y_2O_3–MgO nanopowders (a) and their pore diameter distribution determined by BJH (b) and DFT (c) methods.

Table. Mesostructure characteristics of nanopowders Y_2O_3–MgO analyzed by the nitrogen physisorption

T_{calc}, °C	S_{sp} (BET), m^2/g	D_{np} (BET), nm	D_{pore}, nm		Pore volume, cm^3/g	
			BJH	DFT	BJH	DFT
700	48	29.1	15	14	0.36	0.28
800	34	41.0	23	17	0.29	0.22
900	22	63.4	119	27	0.29	0.15
1000	16	87.2	Not mesured		Not mesured	

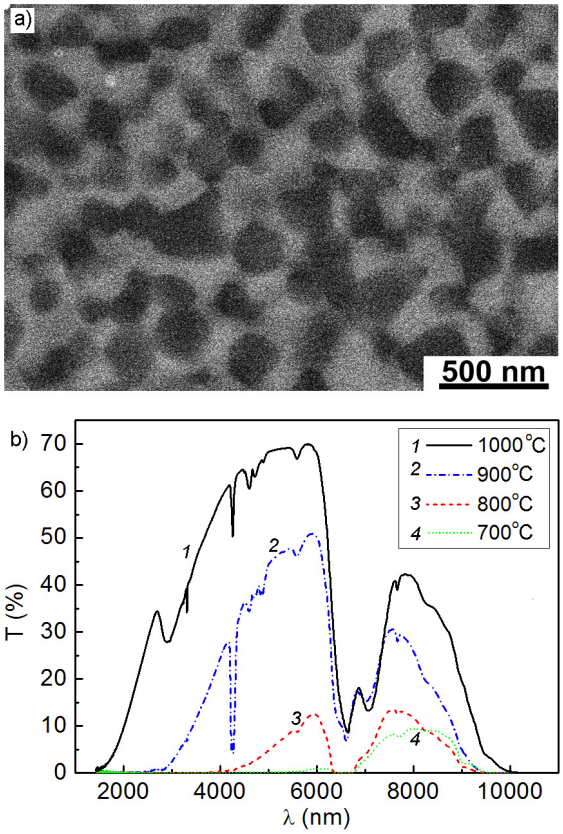

Fig. 6. FESEM of polished Y_2O_3–MgO ceramic surface (a); IR transmittance of SPS sintered Y_2O_3–MgO composite ceramics prepared from nanopowders calcined at 700, 800, 900 and 1000°C for 4 h (b).

Fig. 6a shows FESEM of composite Y_2O_3–MgO ceramics polished surface obtained by SPS from nanopowder calcined at 1000°C. Y_2O_3 (light) and MgO (dark) grains 255 nm in diameter are uniformly distributed in ceramic bulk, pores are not detected.

The optical characteristics of the Y_2O_3–MgO composite ceramics, obtained by the SPS method, improve with an increase in the calcination temperature of the powders (Fig. 6b). Despite the rather low specific surface area of the powder annealed at 1000°C (16 m^2/g), which corresponds to particle size of 87 nm, ceramics, obtained from these powders, show the highest transmittances in the near IR range, about 71 %. In the optical transmission spectra of Y_2O_3–MgO ceramics a wide intense absorption band at the wavelength range of 6–7 μm is observed due to asymmetrical and symmetrical stretching vibration of carboxylate group. This band may be due to the presence of residual carbonates not removed during calcination and sintering.

4. Discussion

According to DTA the precursor, obtained by the glycine-nitrate method with an excess of glycine and nitric acid, contains about 20 % of unreacted components and intermediate reaction products. Subsequent calcining of the powders in air at 600°C should ensure redox reactions, which, according to TEM, is accompanied by the formation of filamentary structures with a diameter of 10 nm (Fig. 2b). It is known that calcination of sol-gel combustion-derived powders at 600°C is sufficient to form 20 nm nanocrystals [14]. When using the glycine-nitrate method with an excess of glycine and nitric acid, the gel fine structure is stabilized due to the release of a large number of gaseous products, incomplete decomposition of the precursor, which complicates mass transfer between particles. When calcining at 600°C for 2 h, the crystalline phases of MgO and Y_2O_3 nucleate, which is confirmed by XRD. However, the growth of crystallites is not observed due to the low diffusion mobility of atoms. The growth of isolated nanocrystals begins at temperatures above 600°C.

Thermogravimetric data indicate that the mass loss after precursor calcination at 1000°C is less than after calcination at 800°C. In addition, when the sample is heated above 600°C, continuous mass gain is observed. This indicates the occurrence of adsorption processes on the surface of the formed nanocrystals. According to FT-IR, the composition of the powders calcined at temperatures of 600, 800, and 1000°C contains carbonate groups, and the intensity of their absorption bands is practically independent of the calcination temperature (Fig. 4b). The lines corresponding to the vibrations of physically adsorbed CO_2 at 2300 cm^{-1} region [24] are absent on the FT-IR spectra of the studied samples, which makes it possible to exclude physical adsorption of CO_2 from consideration. The presence of a wide absorption line with a maximum at 3430 cm^{-1}, corresponding to vibrations of O–H groups, is associated with water adsorption from the atmosphere.

It is known [25] that calcining of Y_2O_3 nanopowders in air at 1000°C leads to the removal of surface carbonate groups. In [26] it was shown that the interaction of CO_2 with MgO nanopowders, prepared through solution-combustion synthesis and ball-milling process, occurs by chemisorption with the formation of a thin surface

layer of $MgCO_3$ on the surface of MgO particles. It can be assumed that when calcining Y_2O_3–MgO composite powders in air, MgO nanoparticles with a high surface intensively trap CO_2.

Suppose that the difference in mass loss between samples calcined at 800 and 1000°C (2.15 %) corresponds to the mass of chemisorbed CO_2 on the surface of MgO nanoparticles. In accordance with the molar ratio $MgO:Y_2O_3 = 0.25$ (1:1 by volume) and reaction (6), we can estimate the mass of magnesium oxide converted to carbonate. According to calculations, about 5 % of the MgO mass in the composite Y_2O_3–MgO powder converts to $MgCO_3$, which corresponds to an adsorption value of 1.17 mmol/g. This is comparable with the value of CO_2 chemisorption by the MgO surface (1.611 mmol/g at 25°C and 1 atm, $S_{sp.}$ (BET) 15 m^2/g) obtained in [26]. According to thermogravimetric data, about 8 % of the mass of MgO is converted to $MgCO_3$.

$$MgO + CO_2 = MgCO_3. \quad (6)$$

On the one hand, the chemisorption of CO_2 can underestimate the specific surface area of powders, since degassing before measurements by the BET method cannot remove CO_2 chemisorbed on the active centers of MgO nanoparticles. On the other hand, after powders calcining at 900°C, additional pores with diameter of 2 to 8 nm are formed (Fig. 5 b, c, Table). The formation of a more developed surface at the nanoscale can be explained by the chemical transformation of MgO into $MgCO_3$, which is accompanied by deformation and an increase in the crystal lattice volume on the surface of nanocrystals. $MgCO_3$ phase was not observed by XRD in calcined powders (Fig. 4a). Thus, in the composition of the Y_2O_3–MgO nanopowders, there is a certain amount of the $MgCO_3$ phase, not fixed by XRD, in the form of nanolayers on the surface of MgO nanocrystals.

Despite the rather low specific surface area of powders calcined at 1000°C (S = 16 m^2/g), the Y_2O_3–MgO ceramics obtained from them demonstrates the best optical quality (Fig. 6). This is due to low agglomeration and a higher crystallinity degree of Y_2O_3 and MgO nanoparticles formed under these conditions. Moreover, the developed surface of MgO nanocrystals additionally activates the sintering process. Apparently, the SPS regimes used in this work do not allow complete removal of residual carbonates, which leads to the appearance of a wide absorption band in the ceramics spectra in the region of 7 μm.

5. Conclusions

Using self-propagating glycine-nitrate synthesis with an excess of glycine and nitric acid, Y_2O_3–MgO nanopowders (1:1 by volume) were synthesized. It has been shown that as-prepared powder contains about 19 % of unreacted components and intermediate reaction products. The formation of isolated nanocrystals starts at calcination temperature above 600°C. Calcination at temperatures from 700 to 1000°C leads to the formation of nanocrystals with diameter of 20 nm and 90 nm, respectively. The specific surface area (BET) of composite powders decreases with increasing calcination temperature from 48 to 16 m^2/g, which is accompanied by a decrease in pore volume. After calcining at 800°C and higher in air atmosphere, intense chemisorption of CO_2 occurs on the surface of nanopowders. As a result, about 5 wt.% MgO is converted to carbonate. Chemical transformation of the surface of magnesium oxide nanocrystals after calcining at 900°C leads to the appearance of additional mesopores with diameter of 2–8 nm.

The optical characteristics of the Y_2O_3–MgO composite ceramics, obtained by the SPS method, improve with an increase in the powders calcination temperature. The highest transmittance (71 %) is observed for ceramics with an average grain size of 255 nm, obtained from powders calcined at 1000°C. Absorption in the region of 6–7 μm may be due to the presence of the $MgCO_3$ phase on the surface of MgO nanocrystals.

Acknowledgements. This work was supported by the National Academy of Sciences of Ukraine within the frame of the Project "Nanoceramics", as well as by the Chinese Academy of Sciences, Special Communication Plan Application Type B for 2018-2019.

References

1. D.C.Harris, L.R.Cambrea, L.F.Johnson et al., *J. Am. Ceram. Soc.*, **96**, 3828 (2013).
2. D.C.Harris, *Infrared Phys. Technol.*, **39**, 185 (1998).
3. D.T.Jiang, A.K.Mukherjee, *J. Am. Ceram. Soc.*, **93**, 769 (2010).
4. S.Xu, J.Li, H.Kou et al., *Ceram. Int.*, **41**, 3312 (2015).
5. C.-H.Chen, J.K.M.Garofano, C.K.Muoto et al., *J. Am. Ceram. Soc.*, **94**, 367 (2011).

6. V.L.Blair, Z.D.Fleischman, L.D.Merkle et al., *Appl. Opt.*, **56**, B154 (2017).
7. A.Iyer, J.K.M.Garofano, J.Reutenaur, *J. Am. Ceram. Soc.*, **96**, 346 (2013).
8. A.Varma, A.S.Mukasyan, A.S.Rogachev et al., *Chem. Rev.*, **116**, 14493 (2016).
9. F.Deganello, A.K.Tyagi, *Progr. Cryst. Growth. Character. Mater.*, **64**, 23 (2018).
10. Ho Jin Ma, Wook Ki Jung, Changyeon Baek, Do Kyung Kim, *J. Eur. Ceram. Soc.*, **37**, 4902 (2017).
11. S.Ghorbani, R.Sh.Razavi, M.R.Loghman-Estarki et al., *J. Clust. Sci.*, **43**, 345 (2017).
12. Shengquan Xu, Jiang Li, Huamin Kou et al., *Ceram. Int.*, **41**, 3312 (2015).
13. Junxi Xie, Xiaojian Mao, Xiaokai Lia et al., *Ceram. Int.*, **43**, 40 (2017).
14. M.Yong, D.H.Choi, K.Lee, *Arch. Metall. Mater.*, **63**, 1481 (2018).
15. S.R.Jain, K.C.Adiga, V.R.Pai Verneker, *Combustion and Flame*, **40**, 71 (1981).
16. A.V.Zhilkina, A.A.Gordienko, N.A.Prokudina et al., *Rus. J. Phys. Chem.*, **A 87**, 674 (2013).
17. P.Melnikov, V.A.Nascimento, L.Z.Z.Consolo et al., *J. Thermal Anal. Calorimetry*, **111**, 115 (2013).
18. Li-Hui Yin, Xu-Ping Liu, Lu-Yao Yi et al., *J. Innovative Opt. Health Sci.*, **10**, 1650052 (2017).
19. Youjin Zhang, Minrui Gao, Kaidong Han et al., *J. Alloys Compd.*, **474**, 598 (2009).
20. S.Stopic, C.Dertmann, G.Modolo, *Metals*, **8**, 993 (2018).
21. Mohammad Khajelakzay, Reza Shoja Razavi, Masoud Barekat, *Trans. Ind. Ceram. Soc.*, **74**, 208 (2015).
22. Anam Ansaria, Abad Alia, Mohd Asifa et al., *New J. Chem.*, **42**, 184 (2018).
23. Feng Chen, Ying-Jie Zhu, Ke-Wei Wang et al., *Current Nanosci.*, **5(3)**, 266 (2009).
24. Gan Song, Xun Zhu Rong, Chen Qiang Liao et al., *Chem. Engin. J.*, **283**, 175 (2016).
25. S.Som, S.K.Sharma, *J. Phys. D: Appl. Phys.*, **45**, 415102 (2012).
26. E.Gutierrez-Bonilla, F.Granados-Correa, V.Sanchez-Mendieta et al., *J. Environ. Sci.*, **57**, 418 (2017).